

## **SOURCE DISTRIBUTION METHOD AND HYDRODYNAMICS COEFFICIENTS OF VESSEL**

Yeak Su Hoe  
Department of Mathematics  
Faculty of Science  
Universiti Teknologi Malaysia

Adi Maimun  
Department of Marine Technology  
Faculty of Mechanical Engineering  
Universiti Teknologi Malaysia

### **ABSTRACT**

*In the present research, fix structure and floating structure such as vessel are studied in terms of hydrodynamics forces and hydrodynamics coefficients. Currently, three-dimensional source distribution method is adopted which taking into account the actual design of fix structure as well as hull form. A curved triangular boundary element is implemented with constant source distribution on each element. Some improvements are adopted in order to solve the singular integration of elements. Gauss-type Laguerre integration as well as cauchy principal value are implemented to solve the Green function numerically. These modification show some improvement of accuracy according to number of panels. Experimental result of Greek passenger ship is compared with present result as well as Frank Close-Fit Method.*

**Keywords:** *Time Domain Ship Simulation, Curved Triangular Boundary Element, Source Distribution Method, Discretization of Element, Green's Function, Singular Integration Method.*

### **1.0 BACKGROUND**

One of the approach for the computation of fluid-structure interaction associated with fixed or floating structures is diffraction theory or potential flow theory. Diffraction theory, as to be known, refers to the inviscid, incompressible and irrotational solution of fluid-structure interaction. In the linear diffraction theory the solution to the fluid-structure problem is solved such that the linearized free-surface boundary condition is satisfied as well as the kinematic boundary condition on the surface of the body and on the sea floor. In addition, the waves caused by the presence of the body or its motion satisfy a radiation condition at far distance from the body.

One of the main limitation of the diffraction theory is the negligence of the effect of viscosity. This discrepancy is obvious when comparison is made between numerical results and experimental result of hydrodynamics coefficients.

## 2.0 GREEN'S FUNCTION METHOD

The time dependence of the fluid motion to be considered here is restricted to simple harmonic motion and, accordingly,  $\Phi$  may be expressed as

$$\Phi = Re[\phi(x, y, z)e^{-i\omega t}] \quad (1)$$

where  $\omega = 2\pi/T$  denotes the frequency of the motion,  $T$  being the period and  $\phi$  denotes the complex potential. The coordinate system  $(x; y; z)$  is referred to still water surface.

The complex potentials must satisfy the Laplacian,

$$\nabla^2 \phi = 0, \quad (2)$$

The kinematic boundary condition on the bottom also must be satisfied,

$$\frac{\partial \phi}{\partial z}(0, y, -h) = 0, \quad (3)$$

where  $h$  denotes the water height. The boundary condition to be applied on the immersed surface in problems considered here will be of the form,

$$\frac{\partial \phi}{\partial n} = v_n, \text{ on } S(x, y, z) = 0, \quad (4)$$

where  $S(x, y, z)$  denotes the surface equation of the body  $V_n$  denotes the specified complex function which represents the magnitude of the normal component of velocity on the immersed surface given by  $V_n = Re[V_n(x, y, z)e^{-i\omega t}]$ . The linearized free surface boundary condition should be satisfied,

$$\frac{\partial \phi}{\partial z}(x, y, 0) - \frac{\omega^2}{g}\phi(x, y, 0) = 0 \quad (5)$$

Finally, in order to insure that the velocity potential has the correct behaviour in the far field, the radiation condition must be fulfilled.

The source distribution produces normal velocities which are discontinuous across the surface  $S$  but if the flow on one side only is of interest, the source distribution appears to be the more convenient method and is applied in the following.

$$\phi = \frac{1}{4\pi} \iint_S f(\epsilon, n, \xi) G(x, y, z; \xi, \eta, \zeta) = dS \quad (6)$$

where  $(\xi, \eta, \zeta)$  denotes a point on  $S$  and  $f(\xi, \eta, \zeta)$  denotes the unknown source distribution.

The integral is to be carried out over the complete immersed surface of the object. The Green's function,  $G(x, y, z; \xi, \eta, \zeta)$  must, in order for the representation in Equation (6) to be valid, satisfy all the boundary conditions of the problem above with the exception of the kinematic condition, Equation (4).

The particular expression for  $G$  appropriate to the boundary-value problem posed is given by Wehausen and Laitone [1].

$$G = \frac{1}{R} + \frac{1}{R'} + 2P.V. \int_0^\infty e^{-\mu d} \frac{(\mu + v) \cosh[\mu(\zeta + d)] \cosh[\mu(z + d)]}{\mu \sinh(\mu d) - v \cosh(\mu d)} J_0(\mu r) d\mu + i2\pi \frac{(k^2 - v^2) \cosh[k(\zeta + d)] \cosh[k(z + d)]}{k^2 d - v^2 d + v} J_0(kr) \quad (7)$$

where,

$$R = [(x - \xi)^2 + (y - \eta)^2 + (z - \zeta)^2]^{1/2},$$

$$R' = [(x - \xi)^2 + (y + \eta)^2 + (z + 2d + \zeta)^2]^{1/2},$$

$$r = [(x - \xi)^2 + (y - \eta)^2]^{1/2} \text{ and}$$

$$v = k \tanh(kd);$$

The solution to the boundary-value problem as given by Equation (6) satisfies Equations (2), (3) and (4). When the kinematic boundary condition on the immersed surface (Equation (4)) is applied, the following integral equation is obtained:<sup>1</sup>

$$-f(x, y, z) + \frac{1}{2\pi} \iint_S f(\xi, \eta, \zeta) \frac{\partial G}{\partial n}(x, y, z; \xi, \eta, \zeta) dS = 2v_n(x, y, z) \quad (8)$$

As usual,  $\frac{\partial G}{\partial n}$  denotes the derivative of the Green's function in the outward normal direction and  $(x, y, z)$  denotes points on  $S(x, y, z) = 0$

### 3.0 NUMERICAL SOLUTION

The integral Equation (8) may be solved numerically with the subdivision of  $S$  into  $N$  curved triangular panels (6 nodes each element) of area  $\Delta S_j$  ( $j = 1, 2, \dots, N$ )

<sup>1</sup> The constant element of source is adopted in order to avoid corner problem.

and identifying as node points the centroid of each panel. As shown in Figure 1, every element consist of 6 nodes in order to produce a curved triangular.

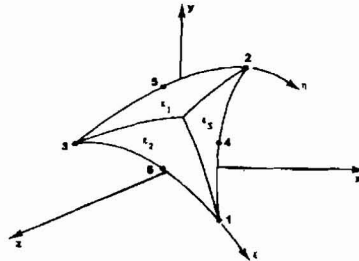


Figure 1 Curved triangular boundary element

The techniques of discretization of the surface of the ship hull adopts procedure employed by Bratanow, et. al [2] with some modification. Every two station will be added a middle station, for instance, according to Figure 2, the station (n+1) is added. The original station offset only include station (n) and (n+2). After the discretization, Equation (8) is replaced by the N equations as below:

$$-f(x_i, y_i, z_i) + \frac{1}{2\pi} \iint_s f(\xi, \eta, \zeta) \frac{\partial G}{\partial n}(x_i, y_i, z_i, \xi, \eta, \zeta) ds = 2v_{ni}(x_i, y_i, z_i) \quad (9)$$

By assuming the source strength function  $f(\xi, \eta, \zeta)$  as constant over each element, the Equation (9) becomes,

$$-f_i = \alpha_{ij} f_j = 2v_{ni}, \quad i, j = 1, 2, \dots, N, \quad (10)$$

where the repeated index denotes summation and

$$\alpha_{ij} = \frac{1}{2\pi} \int_{\Delta s_j} \int \frac{\partial}{\partial n} G(x_i, y_i, z_i, \xi, \eta, \zeta) dS \quad (11)$$

Physically,  $\alpha_{ij}$  denotes the velocity induced at the  $i$ th node point in the direction normal to the surface by a source distribution of unit strength distributed uniformly over the  $j$ th panel. Equation (10) can be solved easily. In order to reduce the computation time, the linear system of Equation (10) will be transformed into block system. The Gauss elimination procedure with block partition will reduce the computation time of CPU significantly.

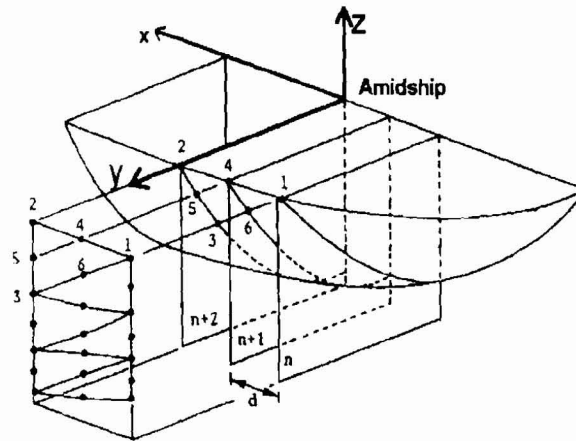


Figure 2 Discretization of ship hull

Following the same procedure, Equation (6) may be written as

$$\phi_i = \beta_{ij} f_j \quad i, j = 1, 2, \dots, N \quad (12)$$

where

$$\beta_{ij} = \frac{1}{4\pi} \iint_{\Delta S_j} G(x_i, y_i, z_i, \xi, \eta, \zeta) dS \quad (13)$$

In order to determine the hydrodynamic pressure on the immersed surface of vessel hull, the Bernoulli's equation is used.

$$P = \rho\omega \operatorname{Re}[i\phi e^{-i\omega t}] - \frac{1}{2} \rho \operatorname{Re}[(\phi_x^2 + \phi_y^2 + \phi_z^2) e^{-2i\omega t}] - \frac{1}{2} \rho [|\phi_x|^2 + |\phi_y|^2 + |\phi_z|^2] - \rho g z. \quad (14)$$

Currently, only the first term is used to calculate the hydrodynamic forces and moments. The forces and moments acting on the immersed surface are obtained by integration of the pressure distribution. The force and moment vector are obtained from the surface integrals

$$F = -\rho\omega \iint_S \operatorname{Re}[i\phi e^{-i\omega t}] n dS \quad (15)$$

$$M = -\rho\omega \iint_S \operatorname{Re}[i\phi e^{-i\omega t}] (r' \times n) dS \quad (16)$$

where  $r'$  denotes the outward position vector extending from the point.

#### 4.0 NUMERICAL CALCULATION OF THE GREEN'S FUNCTION

The third term of Equation (7) can be written as

$$\int_0^{2k} \frac{F_G(\mu)}{\mu \tanh(\mu d) - \nu} d\mu = \int_0^{2k} \frac{F_G(\mu) - F_G(k)}{\mu \tanh(\mu d) - \nu} d\mu + F_G(k) \int_0^{2k} \frac{1}{\mu \tanh(\mu d) - \nu} d\mu. \quad (17)$$

$$\int_{2k}^{\infty} \frac{f_G(\mu)}{\mu \tanh(\mu d) - \nu} e^{-e\mu} d\mu = \int_{2k}^{\infty} \frac{f_G(\mu) - f_G(k)}{\mu \tanh(\mu d) - \nu} e^{-\mu d} d\mu + f_G(k) \int_{2k}^{\infty} \frac{1}{\mu \tanh(\mu d) - \nu} e^{-\mu d} d\mu. \quad (18)$$

The first term in Equation (17) can be calculated using Cauchy principal value. However, the second term in Equation (17) can be numerically expanded in powers of  $\mu - k$  as<sup>2</sup>

$$\frac{1}{\mu \tanh(\mu h) - k \tanh(kh)} = \frac{a-1}{\mu - k} + a_0 + a_1(\mu - k) + a_2(\mu - k)^2 + \dots \quad (19)$$

Equation (18) can be solved using Gauss-type Laguerre integration method. Finally, the surface integration over each triangular element can be written as

$$\int ds = \int_0^1 \int_0^{1-\eta} |G| d\xi d\eta \quad (20)$$

where, Jacobian is

$$|G| = \left| \left( \frac{\partial \vec{r}}{\partial l_2} - \frac{\partial \vec{r}}{\partial l_3} \right) \times \left( \frac{\partial \vec{r}}{\partial l_1} - \frac{\partial \vec{r}}{\partial l_3} \right) \right| \quad (21)$$

The element surface is defined by the position vector

$$\vec{r} = x\vec{i}_2 + y\vec{i}_2 + z\vec{i}_3. \quad (22)$$

The triangular element integration in Equation (20) can be easily calculated using Gauss Quadrature over triangle method based on Reddy and Shippy [3]. According to Equation (7), the singular integration over the first term of Equation

(7),  $\iint_S \frac{1}{R} ds$ , can be solved analytically over each element [4].

<sup>2</sup> In the current programme, the number of expansion is limited to 20

## 5.0 RESPONSE OF FLOATING VESSEL

The theoretical hydrodynamic analysis of the motion of floating bodies relies on the principle of superposition of linear solutions. The formal development begins with the assumption that the amplitude of the waves which excites the motion of a floating body is small, and that the resulting induced motion of the body is also small.

Through linearization, the complex problem under consideration can be decomposed and treated as the sum of six separate problems namely surge, heave, sway, roll, yaw and pitch motion of the floating vessel.

The small amplitude periodic motion of the floating body can be described by

$$X_j = \text{Re}[X_j^o e^{-i\omega t}], \quad j = 1, 2, \dots, 6 \quad (23)$$

$$X_j^o = a\Theta_j^o, \quad j = 4, 5, 6 \quad (24)$$

where  $X_j^o$  ( $j=1,2,3$ ) denotes the complex amplitude of the displacements in surge, heave and sway.  $a$  represents the characteristic dimension of the vessel hull and  $\theta_j^o$  denotes the complex angular amplitudes of the motion in roll, yaw and pitch.

The complex potential for wave interaction with the floating vessel is given by

$$\phi = \sum_{j=0}^7 \phi_j, \quad (25)$$

where,

$\phi_0$  is the complex potential associated with the incident wave,

$\phi_i$  ( $i = 1, 2, \dots, 6$ ) denote the complex potentials associated with the six degrees of freedom of the body, and

$\phi_7$  denotes the complex potential associated with the scattering of the incident wave by the restrained vessel hull.

The below relationships are adopted,

$$\Phi_i(x, y, z, t) = \text{Re}[\phi_i(x, y, z)e^{-i\omega t}] \text{ for } i = 1, 2, \dots, 6 \quad (26)$$

Each of the complex potentials must satisfy the Laplacian,

$$\nabla^2 \phi_i = 0, \quad i = 0, 1, \dots, 7 \quad (27)$$

The kinematic boundary condition on the bottom also must be satisfied,

$$\frac{\partial \phi_i}{\partial z}(0, y, -h) = 0, \quad i = 0, 1, 2, \dots, 7 \quad (28)$$

and the linearized free surface boundary condition,

$$\frac{\partial \phi_i}{\partial z}(x, y, 0) - \frac{\omega^2}{g} \phi_i(x, y, 0) = 0 \quad i = 0, 1, \dots, 7. \quad (29)$$

The hull kinematic boundary conditions to be satisfied on the surface  $S(x, y, z = 0)$  are

$$\frac{\partial \phi_1}{\partial n} = g_1 = -i\omega X_1^0 n_x. \quad (30)$$

$$\frac{\partial \phi_2}{\partial n} = g_2 = i\omega X_2^0 n_y. \quad (31)$$

$$\frac{\partial \phi_3}{\partial n} = g_3 = i\omega X_3^0 n_z. \quad (32)$$

$$\frac{\partial \phi_4}{\partial n} = g_4 = i\omega \Theta_4^0 [y n_z - (d_1 + z) n_y], \quad (33)$$

$$\frac{\partial \phi_5}{\partial n} = g_5 = i\omega \Theta_5^0 [(d_1 + z) n_x + x n_z], \quad (34)$$

$$\frac{\partial \phi_7}{\partial n} = g_6 = i\omega \Theta_6^0 [x n_y - y n_x] \quad (35)$$

$$\frac{\partial \phi_7}{\partial n} = g_7 = -5 \frac{\partial \phi_0}{\partial n}$$

$$= \frac{igH}{2\omega} \frac{1}{\cosh ka} \left[ \cosh ks [ik \cos \beta n_x + ik \sin \beta n_y] + k \sinh ks n_z \right] e^{i(kx \cos \beta + ky \sin \beta + \epsilon_0)} \quad (36)$$

The boundary-value problem defined by Equations (27-36) are similar to previous Equations (2-5), therefore, the solution is defined as

$$\phi_k(x, y, z) = \frac{1}{4\pi} \iint_s f_k(\xi, \eta, \zeta) G(x, y, z; \xi, \eta, \zeta) dS \quad (37)$$

where  $k : 1, 2, \dots, 6$  denotes the six degrees of freedom and  $k = 7$  denotes scattering. The integral equations are also of the form given by Equation (8),

$$- f_k(x, y, z) + \frac{1}{2\pi} \iint_s f_k(\xi, \eta, \zeta) \frac{\partial G}{\partial n}(x, y, z; \xi, \eta, \zeta) dS = 2g_k(x, y, z), k = 1, 2, \dots, 7 \quad (38)$$



where  $g_k$  are given in Equations (30-36) and  $H$  denotes the wave height.

Following the same discretization and numerical procedure, Equation (38) can be written

$$-fk_i + \alpha_{ij} f_{kj} = 2gk_i, k = 1, 2, \dots, 7, j = 1, 2, \dots, N, \quad (39)$$

where  $N$  denotes the number of subdivisions on the immersed surface of the hull.

Equation (39) can be solved using Block Gauss Elimination Method. Subsequently, Equation (37) can be written

$$\phi k_i = \beta_{ij} f_{kj}, k = 1, 2, \dots, 7 \quad i, j = 1, 2, \dots, N \quad (40)$$

where  $\beta_{ij}$  is given by Equation (13).

The linearized form of Bernoulli's equation gives the dynamic pressure on the immersed surface in terms of  $\phi_k$  as

$$P_k = \rho\omega \text{Re} \left[ i\phi_k e^{-i\omega t} \right], \quad k = 1, 2, \dots, 6 \quad (41)$$

for motion in the six degrees of freedom, and for wave interaction with the fixed hull

$$P_{07} = \rho\omega \text{Re} \left[ i(\phi_0 + \phi_7) e^{-i\omega t} \right] \quad (42)$$

The forces and moments caused by the dynamic fluid pressure acting on the immersed surface of the body are determined from expressions similar to Equations (15) and (16),

$$F_{ij} = -\iint_S P_j h_i dS \quad i, j = 1, 2, \dots, 6 \quad (43)$$

$$F_i = -\iint_S P_{07} h_i dS \quad i = 1, 2, \dots, 6 \quad (44)$$

where  $F_i$  denotes the  $i^{\text{th}}$  component of wave excitation force or moment and  $F_{ij}$  denotes the  $i^{\text{th}}$  components of force or moment arising from the  $j^{\text{th}}$  component of ship motion. The functions  $h_i$  are

$$h_1 = n_x, \quad h_2 = n_y, \quad h_3 = n_z$$

$$h_4 = yn_z - (d_1 + z)ny, \quad h_5 = (d_1 + z)n_x - xn_z, \quad h_6 = xn_y - yn_x$$

The excitation force and moment coefficients, respectively, may be represented by the complex coefficients

$$C_j = \frac{F_{j(\text{mac})}}{\rho g a^3 0.5H} e^{i\delta} \quad j = 1, 2, 3 \quad (45)$$

$$C_j = \frac{F_{j(\text{max})}}{\rho g a^4 0.5H} e^{i\delta} \quad j = 4, 5, 6 \quad (46)$$

where  $\delta_j$  denotes the phase shift of the force with respect to the crest of the incident wave. A positive value of  $\delta_j$  denotes a lag.  $a$  denotes half of the ship length.

In terms of forces due to the hull's motion, hydrodynamic coefficients such as added mass and damping coefficients can be calculated as below

$$-M_{ij} - iN_{ij} = \frac{F_{ij}(\max)e^{i\delta}}{\rho\omega^2 a^4 x_j^0} \quad i = 1,2,3 \quad j = 1,2,\dots,6 \quad (47)$$

$$-M_{ij} - iN_{ij} = \frac{F_{ij}(\max)e^{i\delta}}{\rho\omega^2 a^4 x_j^0} \quad i = 4,5,6 \quad j = 1,2,\dots,6 \quad (48)$$

where  $M_{ij}$  and  $N_{ij}$  denote the added mass and damping coefficients, respectively. Equations (47) and (48) can be written as

$$M_{ij} + iN_{ij} = \iint_S \frac{1}{\omega a^3 x_j^0} (-\phi_j^i - i\phi_j^R) h_i ds \quad i = 1,2,3 \quad j = 1,2,\dots,6 \quad (49)$$

$$M_{ij} + iN_{ij} = \iint_S \frac{1}{\omega a^4 \Theta_4^0} (-\phi + i\phi_j^R) h_i ds \quad i = 4,5,6 \quad j = 1,2,\dots,6 \quad (50)$$

## 6.0 NUMERICAL RESULTS

For the purpose of comparison, a rectangular bottom-mounted caisson 100 m by 100 m in plan by 50 m high placed in 100 m of water is studied. Numerical results calculated by Garrison [5] presented for a total of 48, 108 and 192 panels are presented in Table 1. According to Figure 3 and Figure 4, the present results are promising. As shown in Table 1, the present results with 48 panels are more accurate than Garrison's method with 48 panels. Obviously, the present results are closer to results with higher number of panels.

The present method is used for a simple hemisphere floating on the water. The results of calculation is close to results produced by Garrison [5]. However, for the comparison with model experiment, some discrepancy occur due to viscosity and rotational effect of wave. According to Figure 6, the experiment use the model of Greek Passenger vessel as shown in Figure 5. According to Figures 6-9, with proper scaling, results are compared between Frank Close-fit, three dimensional source distribution method as well as experiment. Obviously, the experimental result can not be predicted when the natural frequency is more than 0.5 rad/s. However, when the natural frequency is smaller than 0.5 rad/s, the three dimensional source distribution results are closer to experiment's result. In terms of roll added mass, Figure 7 shows that Frank Close-fit method is more

accurate when natural frequency is bigger than 0.5 rad/s. However, when the natural frequency is smaller than 0.5 rad/s, results produced by three dimensional source method is better than Frank Close-fit method.

As shown in Figure 8, the results calculated by three dimensional source method are smaller than Frank Close-fit method. However, both graphs show the same pattern which have maximum value near to 0.7 rad/s.

According to Figure 9, the damping value calculated by Frank close-fit method is bigger than three dimensional source for natural frequency greater than 1 rad/s.

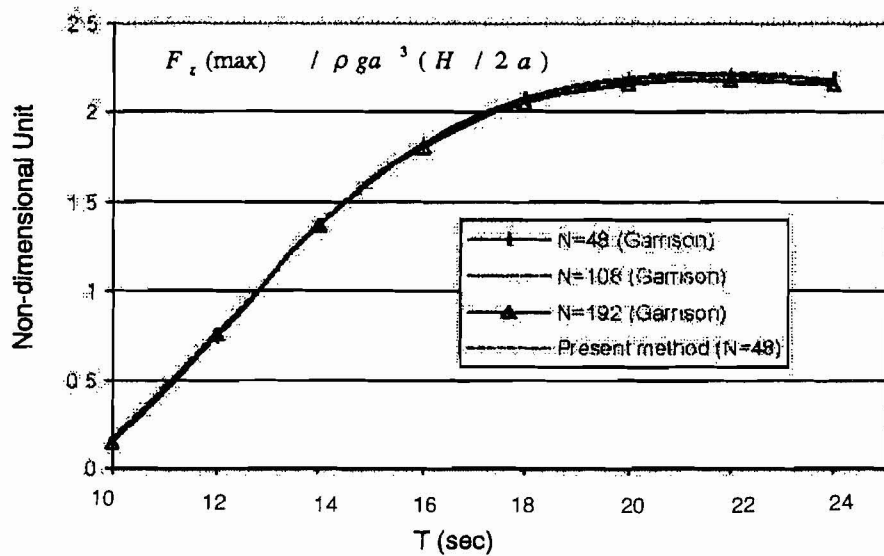


Figure 3 Horizontal Force of a Rectangular Bottom-Mounted Caisson

Table 1 Moment Coefficient,  $M_y(\max)/\rho g a^4 (H/2a)$ , of a Rectangular Bottom-Mounted Caisson.

Period (T)	Garrison (N=48)	Garrison (N=108)	Garrison (N=192)	Present Metod (N=48)
10.0	0.277	0.262	0.264	0.265
12.0	0.140	0.135	0.132	0.133
14.0	0.081	0.075	0.073	0.077
16.0	0.263	0.247	0.240	0.250
18.0	0.382	0.359	0.350	0.363
20.0	0.452	0.424	0.412	0.429
22.0	0.487	0.456	0.444	0.463
24.0	0.500	0.469	0.457	0.476

## 7.0 CONCLUSIONS

For a fix rectangular bottom-mounted caisson, the present method shows some improvement on horizontal force, vertical force as well as moment coefficient

with lower number of panels. In terms of floating vessel, the present method produce a more accurate results of added mass and damping for lower natural frequency which is less than 0.5 rad/s.

### ACKNOWLEDGEMENTS

The financial support of the Universiti Teknologi Malaysia Short Term Research under Project No. 71711, is gratefully acknowledged. The authors also would like to express gratitude to Mr Wong Kim Seng for his valuable assistance.

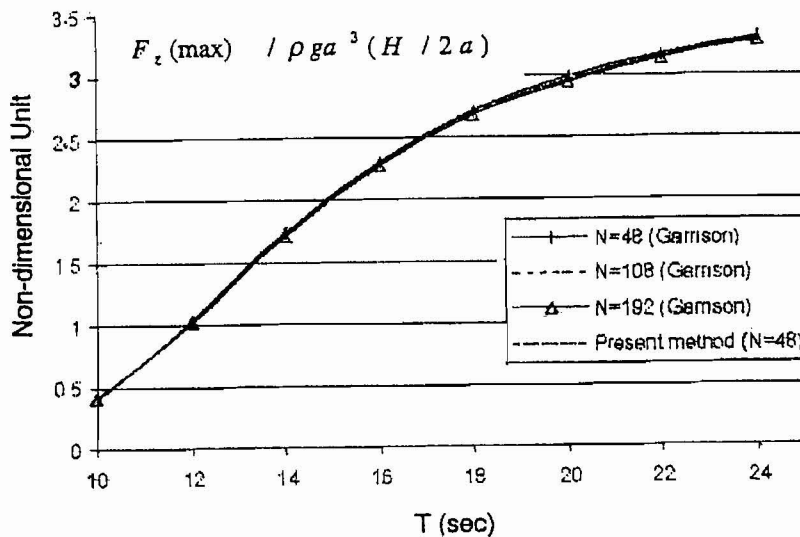


Figure 4 Vertical Force of a Rectangular Bottom-Mounted Caisson

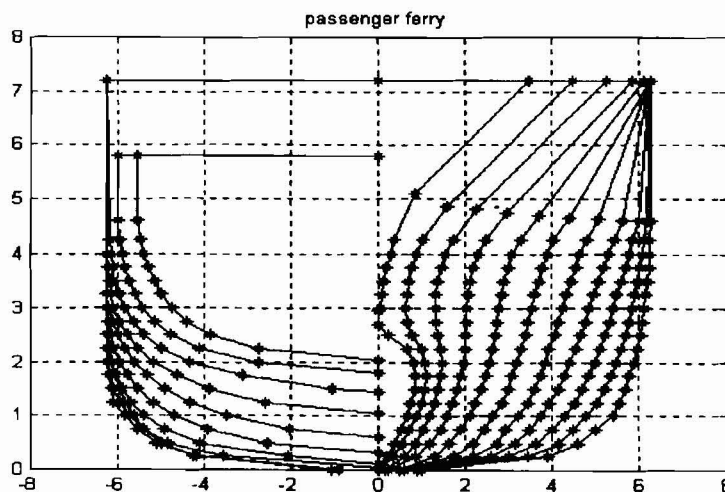


Figure 5 Body Plan of Greek Passenger Vessel

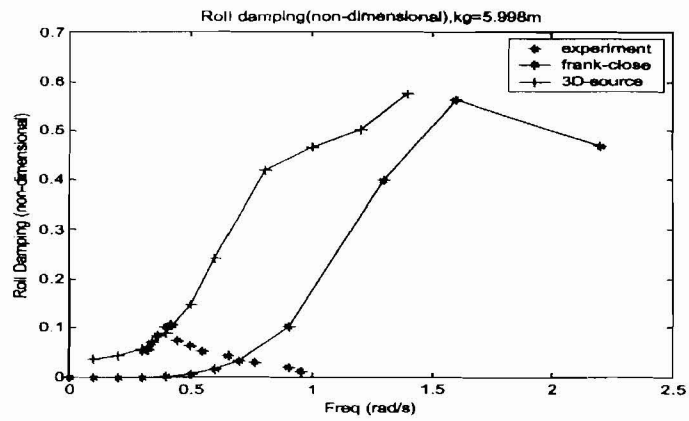


Figure 6 Roll Damping (non-dimensional) with KG=5.998m.

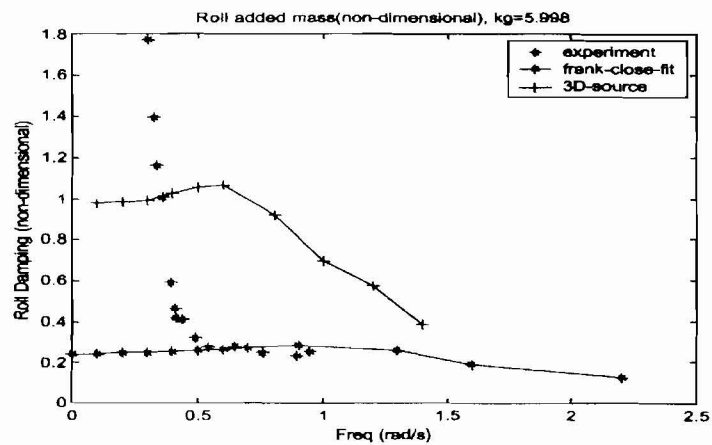


Figure 7 Roll Added Mass (non-dimensional) with KG=5.998m.

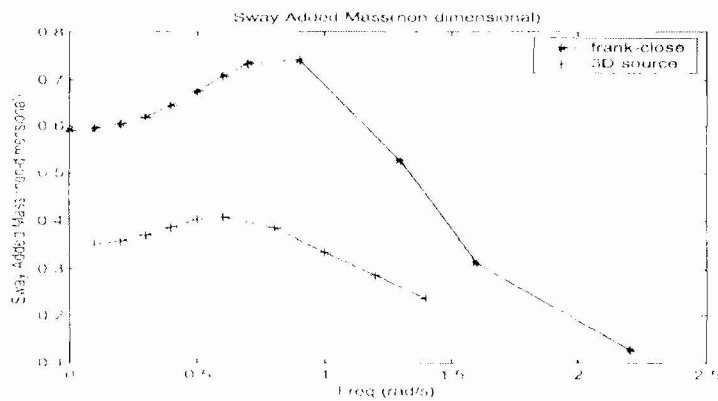


Figure 8 Sway Added Mass (non-dimensional).

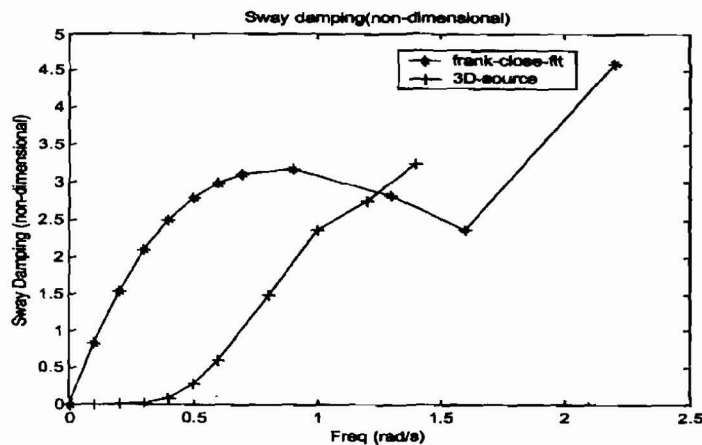


Figure 9 Sway Damping (non-dimensional).

### REFERENCES

1. Wehausen, J.V. and Laitone, E.V. 1960, Surface waves, *Encyclopedia of Physics*, Vol. 9, Springer-Verlag, Berlin.
2. Bratanow, T. Spehert, T & Brebbia, C.A., 1978. Three-Dimensional Analysis of Flows Around Ship Hulls Using Boundary Elements, *Recent Advances in Boundary Element Methods*, Pentech Press, Plymouth, London.
3. Reddy C.T. and Shippy D.J. 1981, Alternative Integration Formulae for Triangular Elements, *Int. J. Numer. Methods in Eng.* vol. 17.
4. Rangogni, R., 1989, Analytical Integration of the Fundamental Solution  $1/R$  Over Panel Boundary Element, *Advances in Boundary Elements, Vol.1: Computations and Fundamentals*, Computational Mechanics Publications, Southampton Boston, U.S.
5. Garrison, C. J., 1978, Hydrodynamic loading of large offshore structures, three-dimensional source distribution methods, *Numerical Methods in Offshore Engineering*, Wiley, London, pp. 87-140.